



## Open Archive Toulouse Archive Ouverte (OATAO)

OATAO is an open access repository that collects the work of Toulouse researchers and makes it freely available over the web where possible.

This is an author-deposited version published in: <http://oatao.univ-toulouse.fr/>  
Eprints ID: 8732

**To link to this article:** DOI: 10.1016/j.electacta.2011.11.029  
URL: <http://dx.doi.org/10.1016/j.electacta.2011.11.029>

**To cite this version:** Ponrouch, Alexandre and Taberna, Pierre-Louis and Simon, Patrice and Palacín, M. Rosa *On the origin of the extra capacity at low potential in materials for Li batteries reacting through conversion reaction.* (2012) *Electrochimica Acta*, vol. 61 . pp. 13-18. ISSN 0013-4686

Any correspondence concerning this service should be sent to the repository administrator: [staff-oatao@listes-diff.inp-toulouse.fr](mailto:staff-oatao@listes-diff.inp-toulouse.fr)

# On the origin of the extra capacity at low potential in materials for Li batteries reacting through conversion reaction

Alexandre Ponrouch<sup>a,b</sup>, Pierre-Louis Taberna<sup>b,c</sup>, Patrice Simon<sup>b,c</sup>, M. Rosa Palacín<sup>a,b,\*</sup>

<sup>a</sup> Institut de Ciència de Materials de Barcelona (ICMAB-CSIC), Campus de la UAB 08193 Bellaterra, Catalonia, Spain

<sup>b</sup> ALISTORE-ERI European Research Institute

<sup>c</sup> Université Paul Sabatier, CIRIMAT, UMR CNRS 5085, Toulouse 31062, France

## A B S T R A C T

The possibility of interfacial storage at low potential for electrode materials reacting through conversion reactions was evaluated. The amount of charge that could be stored through the proposed interfacial mechanism was estimated for a range of different materials and found to be much lower than those observed experimentally. Moreover, the slope of the potential decay and the influence of the current in the extent of stored capacity for experiments carried out in composite electrodes containing  $\text{Co}_3\text{O}_4$  are not consistent with a capacitive-like mechanism. In summary, no evidence for capacitive storage could be found, our results being in agreement with the process taking place at low potential being solely related to electrolyte decomposition.

### Keywords:

Energy storage  
Conversion reactions  
Lithium batteries  
Interfacial storage

## 1. Introduction

The development of lithium based batteries with high energy density is one of the expected breakthroughs in the current quest for energy storage systems with enhanced performance [1,2]. Progress in the study of insertion compounds enabled the development and commercialisation of lithium ion batteries but a paradigmatic shift in energy density will only be achieved with the use of electrodes operating through alternative reaction mechanisms. While materials electrochemically forming alloys with lithium [3] are starting to become a commercial reality, those operating through conversion reactions [4] exhibit promising expectative. The main drawback for those materials is that the large available electrochemical capacity is achieved at the expense of major structural changes in the electrode that are difficult to “buffer”. The electrochemical formation of alloys with lithium has been studied for long and a number of successful strategies [5] have been developed to overcome these intrinsic shortcomings. On the contrary, the study of conversion reaction materials is much more recent and there are still some key issues that deserve understanding at fundamental level such as voltage hysteresis or low coulombic efficiency on the first cycle, before commercial implementation can be realistically discussed.

Conversion reaction is the term applied to define the electrochemical reaction of a binary transition metal compound,  $\text{M}_a\text{X}_b$  ( $\text{M}$ = transition metal,  $\text{X}=\text{O}, \text{S}, \text{F}, \text{P}, \text{N}, \dots$ ) with lithium to yield metallic nanoparticles embedded in a matrix of  $\text{Li}_c\text{X}$ . Due to the full reduction of the transition metal to the metallic state they result in remarkably high capacity values. Moreover, electrochemical capacities exceeding the theoretical value are generally observed [4]. The signature of such additional reversible capacity is a sloping curve at low potentials (generally below 0.8 V vs.  $\text{Li}^+/\text{Li}$ , see Fig. 1A). While decomposition of the electrolyte upon reduction with formation of a gel-like polymeric film which is consumed upon further oxidation has been proved by diverse electrochemical techniques [6–9], an alternative energy storage mechanism termed “interfacial storage” has also been proposed to explain such extra capacity (Fig. 1B). The latter is supported by theoretical calculations [10–12] and based on a two phase capacitive behaviour at the  $\text{M}/\text{Li}_c\text{X}$  interfaces in the reduced electrodes which would allow for the storage of  $\text{Li}^+$  ions on the  $\text{Li}_c\text{X}$  side and electrons on the  $\text{M}$  side. Capacitive and faradaic phenomena being intrinsically different, the aim of the current study was to ascertain whether proof of the existence of such capacitive storage could be achieved in presence of concomitant formation of the gel-like polymeric film through faradaic electrolyte decomposition.

## 2. Experimental

Composite electrodes mimicking industrial technologies were prepared with  $\text{Co}_3\text{O}_4$  as active materials from slurries (65 wt.%

\* Corresponding author at: Institut de Ciència de Materials de Barcelona (ICMAB-CSIC), Campus de la UAB 08193 Bellaterra, Catalonia, Spain.

E-mail address: rosa.palacin@icmab.es (M.R. Palacín).

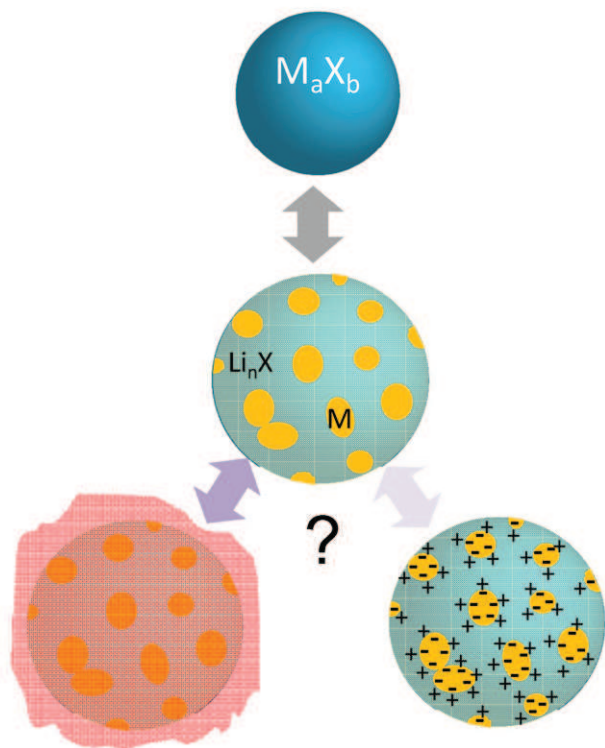
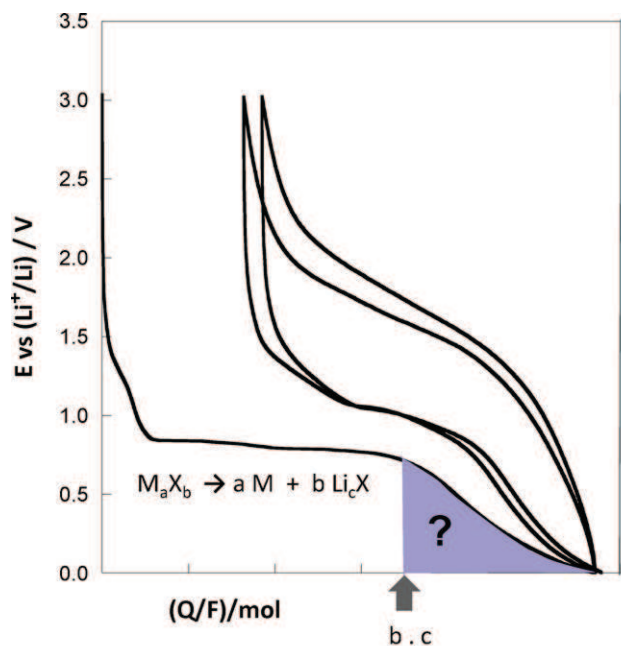


**Fig. 1.** (A) Typical potential versus charge capacity profile curve. Usual values for  $Q/F$  (corresponding to  $b \cdot c$  in Eq. (1)) range between 2 and 8 mol of electrons per mole of  $M_aX_b$  [4]. (B) Schemes of the two proposed redox mechanisms taking place at low potential.

$Co_3O_4$ , 8 wt.% of polyvinylidene fluoride binder (PVDF, Arkema) and 27 wt.% of Super P carbon (Csp hereafter from Timcal) in *N*-methylpyrrolidone (NMP, Aldrich) mixed for 15 h by magnetic stirring with three intermediate 10 min sonication steps [13]. These were tape casted on a 20  $\mu m$  thick copper foil (Goodfellow) with a 250  $\mu m$  Doctor-Blade and further dried at 120  $^{\circ}C$  under vacuum. Once dried, 0.8  $cm^2$  disk electrodes were cut and pressed at 8 t prior to testing.

Electrochemical testing was performed in two electrode Swagelok cells for composite electrodes using a disk of Li metal foil (Chemetall) as counter and reference electrode and 1 M  $LiPF_6$  in EC:DMC 1:1 (LP30, Merck) electrolyte. Electrochemical cycling experiments were made in galvanostatic mode with potential limitation (GCPL) using a Bio-Logic VMP3 potentiostat at very different rates ranging from  $C/10$  to  $10C$  ( $1C$  being one  $Li^+$  inserted in 1 h). Reproducibility was checked by assembly of twin cells.

### 3. Results and discussion

Capacitive electrochemical phenomena are much faster than faradaic processes involving a redox reaction, as illustrated by their respective time constants: seconds for the former and minutes or hours for the latter [14]. Thus, and in order to discriminate between faradaic and capacitive processes in materials reacting through conversion reaction, we decided to evaluate the kinetics of the diverse redox processes taking place in composite  $Co_3O_4$  containing electrodes. The results of galvanostatic cycling at different rates for both electrodes are exhibited in Fig. 2.

Generally speaking, the first reduction of oxides exhibiting a conversion reaction mechanism with respect to lithium exhibits

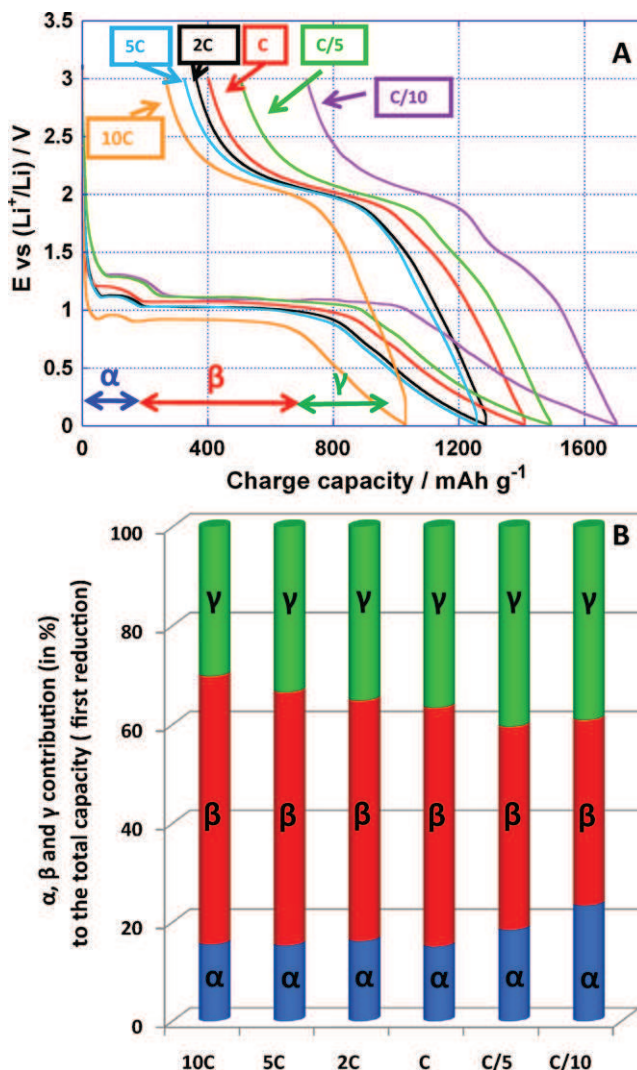


**Fig. 2.** (A) Plot of potential versus charge capacity profile for  $Co_3O_4$  composite electrodes upon the first cycle at different  $C$  rates and (B) plot of the charge capacity percentage for each process (i.e. insertion  $\alpha$ ; conversion  $\beta$  and extra capa  $\gamma$ ) with respect to the total capacity achieved upon the first reduction.

three components: (i) an occasional certain degree of lithium insertion in the structure (which we will denote  $\alpha$ ), (ii) the conversion reaction itself (denoted  $\beta$ ) and (iii) an almost linear potential decay below 1.15 V vs Li<sup>+</sup>/Li (noted  $\gamma$ ) responsible for the extra capacity (see Fig. 1). Fig. 2A exhibits the potential versus capacity profiles for Co<sub>3</sub>O<sub>4</sub> containing electrodes cycled at rates ranging from C/10 to 10C. The total value of the capacity is found to decrease with increasing rate as expected and generally observed in the literature for conversion reaction materials. The relative value of  $\alpha$ , corresponding to the insertion step is found to decrease with increasing the rate in agreement with previous reports suggesting a correlation between the stability of the intercalated phase and the current density [15]. Interestingly, the capacity involved in both  $\beta$  and  $\gamma$  processes is reduced with increasing cycling rate, but this decrease seems to be enhanced for the  $\gamma$  component (extra capacity). This result is confirmed by the plot of the relative value of the  $\alpha$ ,  $\beta$  and  $\gamma$  components with respect to the total capacity (Fig. 2B) achieved upon the first reduction. Indeed, this would mean that the kinetics of the conversion reaction ( $\beta$ ), which corresponds to a faradaic process are faster than that of the  $\gamma$  process occurring at low potential. This is in full agreement with the observed catalytic electrolyte decomposition at these low potentials [16] but does not seem to be consistent with interfacial storage being the main process taking place. Indeed, much faster kinetics should be expected from capacitive processes.

Bearing in mind the two hypothetical mechanisms responsible for the extra capacity at low potential, namely (i) the decomposition of the electrolyte and (ii) the charge storage at the interface between the metallic nanoparticles and the lithiated matrix, it seems straightforward to conclude that in the first case the specific surface of the material (before conversion reaction) would play an important role as the charge associated with the decomposition of the electrolyte is proportional to the surface in contact with the electrolyte. This is in agreement with results from Delmer et al. [17] for RuO<sub>2</sub> with an extra capacity of 31% of the total first discharge for nanoparticles (ca. 60 nm) and 24% for ca. 10  $\mu$ m size particles and also from our previous work on Co<sub>3</sub>O<sub>4</sub> with particle sizes of ca. 35 nm and 1  $\mu$ m exhibiting extra capacities of 35% to 28%, respectively [13].

Capacitive behaviour is characterized by a linear potential decay/increase in the potential–discharge/charge curve, the slope of which is equal to the current divided by the capacitance [18]. The fact that the slope observed upon oxidation is generally larger than upon reduction for conversion reaction materials (see for instance Figs. 1A and 2A) is also in agreement with electrolyte degradation being the main phenomenon accounting for extra capacity at low potentials.

Hypothetical capacitive-like storage at the interface between M and Li<sub>c</sub>X would be difficult to record using conventional techniques since M and Li<sub>c</sub>X are bound to the same current collector and hence exhibit the same potential. Nonetheless we found interesting to estimate the relative amount of charge that could be stored by such a mechanism, which would be proportional to the extent of the M/Li<sub>c</sub>X interface. It is commonly admitted in the literature that metallic nanoparticles with diameter between 2 and 10 nm are formed at the end of a conversion reaction [19,8,20] somewhat independently on the initial particle size. Considering a general conversion process,



Masses of metal M and lithiated matrix (i.e. Li<sub>c</sub>X) obtained at the end of the conversion process can be expressed as follows:

$$m^M = a \cdot M^M \cdot \frac{m_i^{MX}}{M_i^{MX}} \quad (2)$$

$$m^{Li_cX} = a \cdot M^{Li_cX} \cdot \frac{m_i^{MX}}{M_i^{MX}} \quad (3)$$

$m^M$  and  $m^{Li_cX}$  being the mass of metal M and lithiated matrix Li<sub>c</sub>X,  $M^M$  and  $M^{Li_cX}$  being their respective molecular weight, and  $m_i^{MX}$  and  $M_i^{MX}$  being the initial mass and molecular weight of the transition metal compound.

The total volume of these phases can then be expressed as (4) and (5), with  $\rho^u$  being the density of a phase  $u$ :

$$V^M = a \cdot M^M \cdot \frac{m_i^{MX}}{(M_i^{MX} \cdot \rho^M)} \quad (4)$$

$$V^{Li_cX} = a \cdot M^{Li_cX} \cdot \frac{m_i^{MX}}{(M_i^{MX} \cdot \rho^{Li_cX})} \quad (5)$$

Finally, the nanoparticles of metal being considered as spheres with a given radius  $r$ , we can express their total surface at the end of the conversion reaction as follows:

$$S^M = 3 \cdot a \cdot M^M \cdot \frac{m_i^{MX}}{(r \cdot M_i^{MX} \cdot \rho^M)} \quad (6)$$

In addition to the total metallic nanoparticle surface area (Eq. (6)), these simple calculations lead to a general formula to calculate the volume change (given in %) induced by the conversion reaction (7):

$$V_{change}^{\%} = 100 - 100 \times \frac{(V^M + V^{LiX})}{V_i^{MX}} \quad (7)$$

Fig. 3 displays the data obtained solving Eqs. (6) and (7) for most of the materials reported to date reacting through conversion reaction [4] not forming alloys with lithium and considering 1 g of precursor material and 5 nm average metallic particle diameter. All values are plotted with respect to the volume expansion and surface area of metallic nanoparticles per gram of  $M_aX_b$ . We considered fluorides (formation of LiF during conversion): CuF<sub>2</sub>, TiF<sub>3</sub>, VF<sub>3</sub>, CoF<sub>2</sub>, FeF<sub>3</sub>, NiF<sub>2</sub> and CrF<sub>3</sub>; oxides (formation of Li<sub>2</sub>O): Cu<sub>2</sub>O, MnO, CuO, MoO<sub>3</sub>, Fe<sub>3</sub>O<sub>4</sub>, FeO, CoO, Mn<sub>2</sub>O<sub>3</sub>, NiO, Fe<sub>2</sub>O<sub>3</sub>, MoO<sub>2</sub>, Co<sub>3</sub>O<sub>4</sub>, RuO<sub>2</sub>, Cr<sub>2</sub>O<sub>3</sub> and MnO<sub>2</sub>; sulfides (formation of Li<sub>2</sub>S): Cu<sub>2</sub>S, MnS, CuS, FeS, WS<sub>2</sub>, MoS<sub>2</sub>, NiS, CoS<sub>2</sub> and FeS<sub>2</sub>; and also some nitrides (formation of Li<sub>3</sub>N): CrN and Cu<sub>3</sub>N and phosphides (formation of Li<sub>3</sub>P): FeP and Cu<sub>3</sub>P. The low number of phosphides and nitrides results from the scarcity of the density values in [21].

As expected, a general trend appears for the volume change experienced during conversion depending on the oxidation state of X ( $c$ ) which determines the stoichiometry of the binary Li<sub>c</sub>X matrix. The higher  $c$ , the larger the amount of Li<sup>+</sup> reacting in the conversion process per mole of  $M_aX_b$  and hence the larger the expected volume change (cf. Fig. 3). Indeed, the calculated volume changes were found to vary from 11% to 30% for fluorides ( $c = 1$ ), from 65% to 165% for divalent oxides and sulphides ( $c = 2$ ) and from 195% to 235% for phosphides and nitrides ( $c = 3$ ). Additionally, value of  $a/b$  larger than 1 results in lower volume change, as exemplified by the values obtained for Cu<sub>2</sub>O (22%), Cu<sub>2</sub>S (48%) and Cu<sub>3</sub>N (40%) which are much lower than values calculated for other  $M_aO_b$ ,  $M_aS_b$  and  $M_aN_b$  compounds (cf. Fig. 3). While other factors such as cost, availability, operation potential and so on are decisive in terms of estimating the potential interest of electrode materials, basing exclusively in theoretical capacity and volume expansion both trivalent fluorides (e.g. TiF<sub>3</sub>, VF<sub>3</sub>, FeF<sub>3</sub> and CrF<sub>3</sub>) and Fe<sub>3</sub>O<sub>4</sub> appear as most interesting case examples to be studied in detail.

The values of the metallic nanoparticle surface areas for all the above mentioned compounds are depicted in Fig. 3 and range from about ca. 50 to 130 m<sup>2</sup> per gram of  $M_aX_b$ . Interestingly, most compounds develop metallic surface areas around 100 m<sup>2</sup> per gram of  $M_aX_b$ . Coming back to the experimental extra capacity values

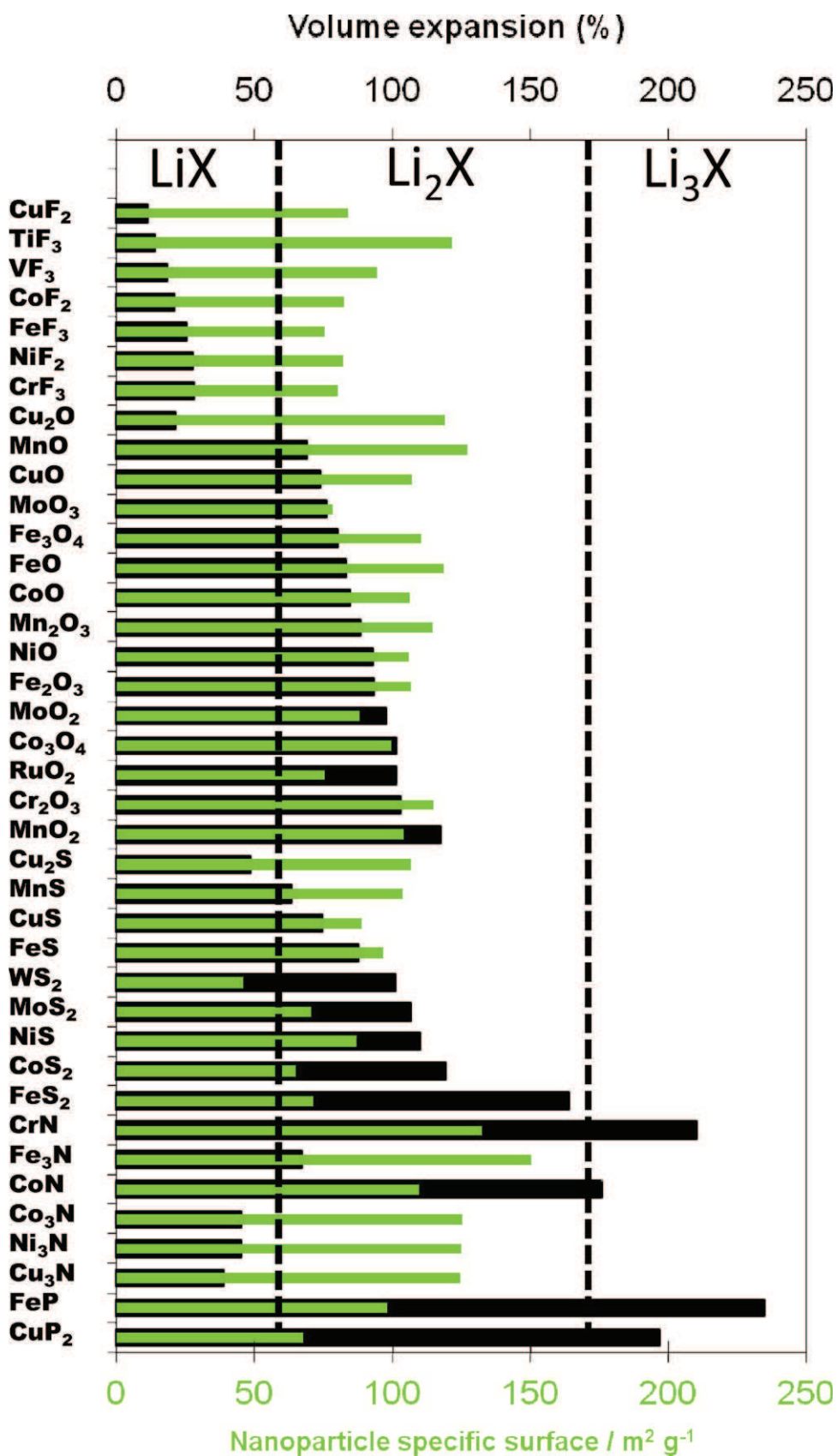
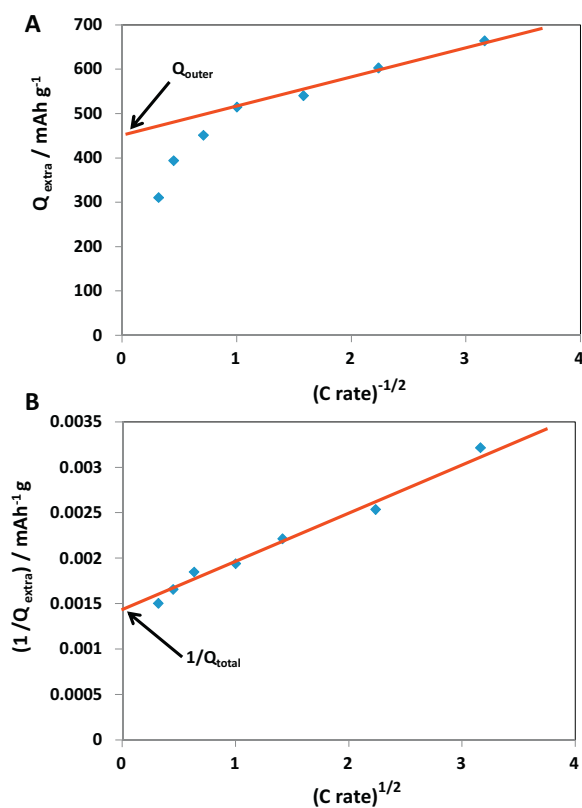


Fig. 3. Plot of volume change percentages (black scale and bars) and M nanoparticles surface area (per  $M_aX_b$  unit mass; green scale and bars) after conversion reaction.



**Fig. 4.** Plots of (A)  $Q_{extra}$  versus  $(C \text{ rate})^{-1/2}$  and (B)  $1/Q_{extra}$  versus  $(C \text{ rate})^{-1/2}$ . Red lines are linear extrapolation of the capacity at infinitely fast and slow  $C$  rates in (A) and (B), respectively.

observed for  $\text{Co}_3\text{O}_4$  (Fig. 2A), are ca.  $600 \text{ mAh g}^{-1}$ , corresponding to  $2160 \text{ C g}^{-1}$ . This capacity being achieved between 1 and 0 V vs  $\text{Li}^+/\text{Li}$ , the charge stored at the interface would be  $2160 \text{ F g}^{-1}$ . Thus, if only interfacial storage at the  $\text{Co}/\text{Li}_2\text{O}$  interface was responsible for the extra capacity and taking into account that  $100 \text{ m}^2$  of metallic cobalt nanoparticles per gram of  $\text{Co}_3\text{O}_4$  are produced at the end of the conversion reaction, the interfacial capacitance value would be  $2160 \mu\text{F cm}^{-2}$ . Knowing that standard maximum value for the double layer specific capacitance at the surface of a metal is about ca.  $30 \mu\text{F cm}^{-2}$  [18], this value is surprisingly high (70 times larger than double layer storage capacity). Thus, it seems straightforward to conclude that if interfacial storage at the  $\text{M}/\text{Li}_c\text{X}$  takes place, it would only account for a small percentage of the experimentally observed capacity, the rest being either fully related to electrolyte decomposition or other processes involving a charge transfer.

It is worth mentioning that similar considerations led, about 40 years ago, to the conclusion that double layer charging contribution was negligible with respect to the very large capacities observed for  $\text{RuO}_2$ ,  $\text{IrO}_2$ , etc. cycled in aqueous acidic solution [22,18]. Indeed, even if a capacitive behavior (i.e. constant current with linear sweep of the potential) was observed in those cases, the obtained capacities are about 10–100 times larger than capacities achievable with accumulation of charge at the double layer interface. Furthermore, Ardizzone et al. demonstrated that the capacitive behavior of  $\text{RuO}_2$  in acidic solution is not only governed by surface processes [23]. Indeed, by extrapolating the value of the charge at infinitely slow and fast sweep rates they were able to discriminate between bulk and surface contribution to the capacities recorded and demonstrated a significant contribution of the bulk of the material. Later on, this demonstration led to the better comprehension of the

charge storage of  $\text{RuO}_2$  involving faradaic reactions with diffusion of protons through the bulk of the material [18].

Fig. 4A displays the plots of the extra capacity (denoted  $Q_{extra}$  thereafter) versus  $(C \text{ rate})^{-1/2}$ . Fig. 4B displays the plots of  $1/Q_{extra}$  versus  $(C \text{ rate})^{-1/2}$ . Similar plots were proposed by Ardizzone et al. [23] in order to evaluate the surface charge (denoted  $Q_{outer}$ ), the total charge (called  $Q_{total}$ ) and the charge related to the bulk contribution of the capacity (called  $Q_{inner}$ ). This was done by extrapolating the value of the capacity at infinite  $C$  rate in Fig. 4A ( $Q_{outer}$ ), by extrapolating the value of the capacity at an infinitely slow  $C$  rate in Fig. 4B ( $1/Q_{total}$ ). Finally  $Q_{inner}$  can be evaluated according to Eq. (8):

$$Q_{inner} = Q_{total} - Q_{outer} \quad (8)$$

From Fig. 4A and B,  $450 \text{ mAh g}^{-1}$  and  $710 \text{ mAh g}^{-1}$  can be estimated for  $Q_{outer}$  and  $Q_{total}$ , respectively. Therefore,  $Q_{inner}$  is ca.  $260 \text{ mAh g}^{-1}$ , representing about 37% of the total extra capacity. This demonstrates the involvement of a kinetically limited process. As previously discussed, the kinetic limitation in the case of  $\text{RuO}_2$  cycled in acidic solution is due to the diffusion of proton through the bulk of the electrode. In the case of  $\text{Co}_3\text{O}_4$  cycled in a non aqueous electrolyte it would be surprising that a kinetically limited process can occur during an interfacial storage as no mass transport is involved. By contrast, the formation of a polymeric film at the surface of the electrode by decomposition of the electrolyte (SEI formation) will obviously be kinetically limited by the diffusion of the electroactive electrolyte species that will decompose at the interface.

#### 4. Conclusions

In this study we evaluated the possibility of interfacial storage at low potential for electrode materials reacting through conversion reactions forming  $\text{M}/\text{Li}_c\text{X}$  composites at the end of reduction. While this would be hardly measurable experimentally within a single electrode, the slope of the potential decay and the influence of the current in the extent of stored capacity do not seem to be consistent with a capacitive-like mechanism. Also, simple geometrical calculations indicate that interfacial storage would only account for a very small percent of the total extra capacity value. These calculations have been generalized to all materials reacting through conversion reactions which are compared in terms of volume expansion and specific surface of metallic nanoparticles at the end of reduction. Bulk and surface processes contribution to capacity has been ascertained using the method reported in [23]. In summary, our results indicate that interfacial storage, if any, would be negligible with respect to electrolyte decomposition to account for the extra capacity observed at low potential in conversion reaction materials.

#### Acknowledgements

We acknowledge Ministerio de Ciencia e Innovación for grant MAT2011-24757 and are grateful to ALISTORE-ERI members for helpful discussions.

#### References

- [1] M.R. Palacín, Chem. Soc. Rev. 38 (2009) 2565.
- [2] M. Armand, J.M. Tarascon, Nature 451 (2008) 652.
- [3] C.M. Park, J.H. Kim, H. Kim, H.J. Sohn, Chem. Soc. Rev. 39 (2010) 3115.
- [4] J. Cabana, L. Monconduit, D. Larcher, M.R. Palacín, Adv. Mater. 22 (2010) E170.
- [5] D. Larcher, S. Beattier, M. Morcrette, K. Edström, J.C. Jumas, J.M. Tarascon, J. Mater. Chem. 17 (2007) 3759.
- [6] G. Gachot, S. Grugeon, M. Armand, S. Pilard, P. Guenot, J.M. Tarascon, S. Laruelle, J. Power Sources 178 (2008) 409.
- [7] S. Grugeon, S. Laruelle, L. Dupont, J.-M. Tarascon, Solid State Sci. 5 (2003) 895.

- [8] S. Grugeon, S. Laruelle, R. Herrera-Urbina, L. Dupont, P. Poizot, J.-M. Tarascon, *J. Electrochem. Soc.* 148 (2001) A285.
- [9] M. Dollé, P. Poizot, L.-J. Dupont, M. Tarascon, *Electrochem. Solid-State Lett.* 5 (2002) A115.
- [10] P. Balaya, A.J. Bhattacharyya, J. Jamnik, Y.F. Zhukovskii, E.A. Kotomin, J. Maier, *J. Power Sources* 159 (2006) 171.
- [11] J. Jamnik, J. Maier, *Phys. Chem. Chem. Phys.* 5 (2003) 5215.
- [12] Y.F. Zhukovskii, P. Balaya, E.A. Kotomin, J. Maier, *Phys. Rev. Lett.* 96 (2006) 058302.
- [13] A. Ponrouch, M.R. Palacín, *J. Power Sources* 196 (2011) 9682.
- [14] P. Simon, Y. Gogotsi, *Nat. Mater.* 7 (2008) 845.
- [15] D. Larcher, G. Sudant, J.-B. Leriche, Y. Chabre, J.-M. Tarascon, *J. Electrochem. Soc.* 149 (2002) A234.
- [16] S. Laruelle, S. Grugeon, P. Poizot, M. Dollé, L. Dupont, J.-M. Tarascon, *J. Electrochem. Soc.* 149 (2002) A627.
- [17] O. Delmer, P. Balaya, L. Kienle, J. Maier, *Adv. Mater.* 20 (2008) 501.
- [18] B.E. Conway, *Electrochemical Supercapacitors: Scientific Fundamentals and Technological Applications*, Kluwer, Norwell, MA, 1999.
- [19] P. Poizot, S. Laruelle, S. Grugeon, L. Dupont, J.-M. Tarascon, *Nature* 407 (2000) 496.
- [20] B. Varghese, M.V. Reddy, Z. Yanwu, C.S. Lit, T.C. Hoong, G.V. Subba Rao, B.V.R. Chowdari, A.T.S. Wee, C.T. Lim, C.-H. Sow, *Chem. Mater.* 20 (2008) 3360.
- [21] D.R. Lide, *Handbook of Chemistry and Physics*, 84th ed., CRC Press LLC, New York, 2003.
- [22] S. Trasatti, G. Buzzanca, *J. Electroanal. Chem.* 29 (1971) 1.
- [23] S. Ardizzone, G. Fregonara, S. Trasatti, *Electrochim. Acta* 35 (1990) 263.